島根大学学術情報リポジトリ
SWAN
Shimane University Web Archives of kNowledge

Title

Dermal absorption of gallium antimonide in vitro and pro-inflammatory effects on human dermal fibroblasts

Author(s)

Fujihara J., Nishimoto N.

Journal

Toxicology in Vitro Volume 71, 2021, 105064

Published

2021

URL（The Version of Record）

https://doi.org/10.1016/j.tiv.2020.105064

この論文は出版社版でありません。
引用の際には出版社版をご確認のうえご利用ください。

This version of the article has been accepted for publication,
but is not the Version of Record.

Dermal absorption of gallium antimonide *in vitro* and pro-inflammatory effects on human dermal fibroblasts

Author names and affiliations.

Junko Fujihara[a], Naoki Nishimoto[b]

[a]Department of Legal Medicine, Shimane University Faculty of Medicine, 89-1 Enya, Izumo, Shimane 693-8501, Japan

[b]Department of Research Planning and Coordination, Shimane Institute for Industrial Technology, 1 Hokuryo, Matsue, Shimane 690-0816, Japan

Corresponding author.

Junko Fujihara

E–mail address: jfujihar@med.shimane-u.ac.jp (J. Fujihara)

Abstract

Gallium antimonide (GaSb) is a group III-V compound semiconductor with a comparatively narrow band gap energy (0.73 eV at 300 K) that allows efficient operation in the near-infrared region. This property may be useful in developing new biomedical instruments such as epidermal optoelectronic devices. The present study investigated the absorption of GaSb in pig skin *in vitro* for 24 h using Franz cells. A donor solution was prepared by soaking GaSb thin films in synthetic sweat. The results showed that both gallium and antimony penetrated the skin, and permeation and resorption occurred for gallium. Histopathological findings showed no inflammatory responses in pig skin exposed to GaSb for 24 h. Cytotoxicity was significantly elevated after 3 and 7 days, and pro-inflammatory cytokines and IL-8 levels were low after 1 and 3 days but elevated 7 days following the direct culturing of human dermal fibroblasts (HDF) on GaSb thin films. These results demonstrate that the short-term cytotoxicity and pro-inflammatory effect of GaSb on HDF were relatively low.

Keywords: Gallium antimonide; Thin film; Franz diffusion cell; Skin permeation; Skin penetration; Pro-inflammatory response

1. Introduction

Recently, semiconductor materials are used for epidermal and E-skin devices (Li et al., 2017; Jung et al., 2018). These devices have been applied for long-term and continuous physiological monitoring. Li et al. (2017) described the application of an epidermal inorganic optoelectronic device using gallium arsenide (GaAs) and silicon materials to measure blood oxygen levels. Jung et al. (2018) developed an optoelectronic device using aluminum indium gallium phosphide (AlInGaP) and applied it to monitor blood flow in the skin.

Application of epidermal optoelectronic devices using Gallium antimonide (GaSb)-based materials can also be expected. GaSb is a group III-V compound semiconductor with a comparatively narrow band gap of 0.73 eV at 300 K, which allows efficient operation in the near-infrared (NIR) region (Dutta et al., 1997). Since biological materials transmit NIR light well, devices operating in the NIR region would be useful for biological applications.

Gallium is likely to irritate the eyes, skin, and mucous membranes and suppress bone marrow function (Ivanoff et al., 2012), and chronic exposure to antimony causes skin lesions called “antimony spots” (Sundar and Chakravarty, 2010). Although the dermal absorption of metals such as platinum (Franken et al., 2015a), palladium (Crosera

et al., 2018), nickel (Crosera et al., 2016), cobalt, chromium (Larese Filon et al., 2007), CdTe/CdS quantum dots (Nastiti et al., 2019), as well as ZnO (Gamer et al., 2006), TiO_2 (Crosera et al., 2015), and Al_2O_3 (Mauro et al., 2019) nanoparticles have been investigated *in vitro*, the dermal absorption and skin affinity of GaSb remain unknown. Investigating the dermal absorption and skin affinity of GaSb is important not only for E-skin applications but also to evaluate occupational exposure. Therefore, the present study aimed to investigate the dermal absorption of GaSb and its toxicity to human dermal fibroblasts (HDF) *in vitro*.

2. Materials and Methods

2.1. Reagents

All reagents used in this study were of analytical grade. Sodium chloride (NaCl) (99.5 %), lactic acid (92 %), urea (99 %), concentrated nitric acid (HNO_3) (60 %), hydrogen peroxide (H_2O_2) (30 %), concentrated hydrochloric acid (HCl) (35 %), potassium iodide (KI) (99.0 %), sodium tetrahydroborate ($NaBH_4$) (99.5 %), sodium hydroxide (NaOH) (97.0 %), phosphate-buffered saline (PBS), gallium (1000 mg/L), and antimony (1000 mg/L) standard solutions were purchased from Fujifilm Wako Pure Chemical Corporation (Osaka, Japan). Standards and other reagents were diluted in Milli-

Q water (> 18 mΩ, Merck Millipore, Burlington, MA, USA).

2.2. Growth of GaSb thin films

GaSb thin films (Fig. 1a) were prepared by RF magnetron sputtering (HSR-351L; Shimadzu Industrial Systems, Otsu, Japan) at 0.5 Pa under an argon atmosphere on a quartz substrate (10 mm × 10 mm × 0.5 mm). The growth temperature and growth time were 600 °C and 30 min, respectively. The gallium content x in Ga_xSb_{1-x} thin film and the film thickness were 0.6 and 370 nm, respectively (Nishimoto and Fujihara, 2020).

2.3. GaSb thin films dissolution in synthetic sweat

Synthetic sweat was prepared using 0.5 % NaCl, 0.1 % lactic acid, and 0.1 % urea in Milli-Q water as described previously (Larese Flion et al., 2008); pH was adjusted to 4.0. Larese Flion et al. (2008) suggested that the actual pH of human skin is in the range of 4.0–5.5. Therefore, in the present study, the pH of artificial sweat was adjusted to 4.0. GaSb thin films were immersed in 10 mL of synthetic sweat at room temperature for 4 days to create the donor solution for the Franz diffusion cell.

2.4. Pig skin

Pig abdominal full-thickness skins (n = 2) for research use (DARD, Tokyo, Japan) were stored at -70 °C until the experiment. Before starting experiments, subcutaneous fat was removed from thawed pig skin, which was then cut into 3 cm × 3 cm and clamped between the donor and receptor chambers of vertical Franz diffusion cells (PermeGear, Somerville, NJ, USA) (Fig. 1b).

The OECD guidelines recommend the use of split-thickness human skin (OECD, 2004). The SCCS guidelines state that "since it is technically more difficult to obtain intact split-thickness skin, this could justify the use of full-thickness skin for pig skin." (SCCS, 2010). Moreover, Mauro et al. (2019) suggested that using full-thickness skin makes a comparison with other *in vitro* studies on metal permeation possible. In fact, previous studies regarding dermal absorption of metals used full-thickness skins (Crosera et al., 2016; Franken et al., 2015a; Gamer et al., 2006; Larese Filon et al., 2007; Mauro et al., 2019; Nastiti et al., 2019). Franken et al. (2015b) reported that full-thickness skin usage could simulate actual workplace conditions when considering exposure. Therefore, full-thickness skins were used in the present study.

2.5. Electrical resistance measurement

A previous study reported that skin samples with a specific resistance of < 35

kΩ /cm^2 were considered damaged and could not be used for diffusion cell studies (Tang et al., 2002). To test the skin quality, the skin electrical resistance was measured according to previous reports (Tang et al., 2002) using a PM7a digital multimeter (Sanwa electric instrument Co., Ltd.. Tokyo, Japan). The skin was clamped between the donor and receptor chambers of Franz diffusion cells, and PBS was added to the donor and receptor chamber. One electrode was immersed in the donor chamber above the skin, and the other electrode was inserted into the receptor chamber via the sidearm. The electrical resistance of the two pig skins exceeded 35 kΩ /cm^2.

2.6. In vitro diffusion system

According to the SCCS guideline, the percutaneous/dermal absorption process can be divided into three steps: 1) penetration, which is the entry of a substance into a particular layer or structure such as the entrance of a compound into the stratum corneum; 2) permeation, which is the penetration through one layer into another, which is both functionally and structurally different from the first layer; and 3) resorption, which is the uptake of a substance into the vascular system (lymph and/or blood vessel), which acts as the central compartment (SCCS, 2010).

Percutaneous absorption was assessed using the Franz method (Franz, 1975).

The donor solution (1 mL) was placed in the donor chamber. Thereafter, a mean volume of 12 mL of receptor solution (PBS) was placed in the receptor compartment and maintained at 32 °C (physiological temperature under normal conditions) with stirring using a magnetic stirrer bar. Portions (1 mL) of receptor solution were removed at 1, 3, 6, and 24 h and diluted with 2 mL of 1N HNO_3. Each portion of the receptor solution was immediately replaced with 1 mL of PBS. The exposed area was 1.77 cm^2, and the thickness was 2 mm. All experiments were conducted in triplicates for each sample (6 samples from 2 donors). Levels of gallium and antimony in the donor solution (before and after exposure), receptor solution, exposed skin, and wash solutions of skin following 24h exposure as decribed below were determined.

2.7. Skin digestion after exposure

Skin exposed for 24 h was washed three times with 5 mL of PBS to remove residual gallium and antimony from the surface. The skin (ca. 0.3 g) was cut into pieces and digested with 5 mL of concentrated HNO_3 for 1.5 h at 65 °C using a DigiPREP Jr heating block acid digestion system (GL Sciences, Tokyo, Japan). After adding 2 mL of 30 % H_2O_2 to the digested sample, the mixture was heated at 95 °C for 2 h, and the digested sample was diluted to 40 mL with Milli-Q water.

2.8. Analyses of gallium and antimony

The gallium concentrations were measured by a microwave plasma-atomic emission spectrometer (MP-AES) using Agilent 4200 MP-AES (Agilent Technologies, Santa Clara, CA, USA) equipped with an Inert One Neb nebulizer and a double-pass glass cyclonic spray chamber (Agilent Technologies) as previously described (Nishimoto et al., 2017). The total antimony concentration was determined by hydride generation (HG) - MP-AES using an MP-AES system coupled to a multimode sample introduction system (MSIS) (Agilent Technologies) according to our previously described method (Fujihara and Nishimoto, 2020). Before analysis, antimony species in the calibration standards and samples (2.5 mL) were reduced with 20 % KI (500 µL) and acidified with 1 N HCl (2 mL) for at least 30 min. The reduced samples and fresh 3 % w/v $NaBH_4$/0.2 % w/v NaOH were infused into the MSIS using a peristaltic pump. Antimony was detected as gaseous antimony trihydride (SbH_3; stibine). Five calibration standards over the range of 0–1000 µg/L were used for both gallium and antimony analysis. Method validation of the gallium and antimony analysis was performed. Method evaluation and recovery of gallium and antimony in a skin sample spiked with gallium and antimony solution are shown in Table 1. Good accuracy and precision were obtained.

2.9. Histopathological evaluation

Small portions of exposed pig skin were fixed in 10 % formalin and stained with hematoxylin and eosin (HE) for histopathological evaluation. Bright-field images were obtained using an EVOS FL cell fluorescence microscope cell imaging system (Thermo Fisher Scientific Inc., Waltham, MA, USA) at × 40 magnification.

2.10. Cell culture

Human dermal fibroblast cells (Toyobo, Osaka, Japan) were cultured in HDF growth medium at 37 °C under a 5 % CO_2 atmosphere at > 95 % humidity. The passage number was five.

2.11. MTT assays

The viability of HDF cells on the top surface of the GaSb thin films was determined using 3-(4,5-dimethylthiazol-2-yl)-2,5-diphenyltetrazolium bromide (MTT) cell count kits (Nacalai Tesque, Kyoto, Japan). Cells (1×10^4 /well) were seeded on GaSb thin films in 24-well plates. Control cells were seeded on quartz. Cell proliferation was assessed after 1, 3, and 7 days of incubation using MTT assays, as we previously

described (Nishimoto and Fujihara, 2019). The MTT solution (10 μL) was added to each well, incubated for 4 h, and then decanted. The cells were incubated with a crystal-dissolving solution (100 μL) at 37 °C, and then absorbance at 570 (test) and 690 (reference) nm was measured using a microplate spectrophotometer (Thermo Fisher Scientific Inc.).

2.12. Measurement of IL-8

Cells (1×10^4 /well) were seeded on GaSb thin films in 24-well plates, then culture supernatants of HDF cells were collected at 1, 3, and 7 days of incubation. The production of IL-8 was evaluated using an IL-8 ELISA Kit (Proteintech Group, Rosemont**,** IL, USA), as described by the manufacturer. Absorbance at 450 nm was measured using a Multiskan™ GO Microplate Spectrophotometer (Thermo Fisher Scientific Inc.).

2.13. Statistical analysis

Data are shown as means ± standard deviation (SD). The Mann–Whitney U test was employed to detect differences between control and treated groups in the MTT assay. As for the IL-8 levels, differences between control and treated groups were analyzed

using Dunnett's test. Data were statistically analyzed using the BellCurve program for Excel (Social Survey Research Information Co., Ltd. Tokyo, Japan).

3. Results

3.1. Frantz diffusion cell assays in vitro

Figure 2 shows the permeation profiles of gallium and antimony after exposure to the donor solution, which was prepared by immersing the GaSb thin films in synthetic sweat. The GaSb was unstable in synthetic sweat, and all of it dissolved in the solution. Both gallium and antimony in the test solution might have been in the ionic form. The permeated gallium concentration increased up to 24 h. In contrast, antimony in the receptor solution was not detectable after 24 h. We assayed the gallium and antimony amounts retained inside the pig skin after 24 h of exposure (Fig. 3). The gallium concentration was below the LOD in pig skin after 24 h of exposure, whereas 1.01 μg ± 0.24/cm^2 of antimony was retained inside the skin. Table 1 shows the mass balance of gallium and antimony calculated from the donor solution (before and after exposure), receptor solution, exposed skin, and wash solutions of skin after 24 h of exposure. A good mass balance was achieved for both gallium and antimony.

3.2. Histopathological findings

Figure 4 shows histopathological images of pig skin exposed to GaSb for 24 h and control skin stained with HE. Acanthosis, stratum corneum detachment from the epidermis, and neutrophil infiltration of the stratum corneum were not evident.

3.3. Effects of GaSb on HDF viability

The viability of HDF cultured directly on the top of the GaSb thin films for 7 days was performed (Fig. 5). The cell viability was significantly lower for HDF exposed to GaSb for 3 and 7 days than in the control group.

3.4. Effect of GaSb on pro-inflammatory responses in HDF cells

The levels of IL-8 in supernatants of HDF cell cultures grown on the surfaces of GaSb thin films were assayed. IL-8 levels were significantly elevated only after 7 days when compared to those of control cells (Fig. 6).

4. Discussion

The dermal absorption of chemicals has been investigated in pig skin as an alternative to human skin (Bronaugh et al., 1982; Sato et al., 1991; Simon and Maibach,

2000). Here, we assayed the dermal absorption of GaSb in pig skin for 24 h using Franz diffusion cells. Preliminarily, we performed Frantz diffusion cell assay by applying GaSb thin films directly on the skin; the thin films were pressed by weight to avoid floating, and 1mL artificial sweat was added to evaluate dermal absorption of GaSb, assuming application as an E-skin device. However, both gallium and antimony in receptor fluids and skin were below the detection limit (data not shown). To investigate the dermal absorption of gallium and antimony, donor solutions were prepared by soaking GaSb thin films in 10 mL of synthetic sweat, and 1mL was applied to donor cells. The results showed that both gallium and antimony penetrated the skin, and permeation and resorption occurred for gallium (Fig. 2 and 3). A good mass balance was achieved for both gallium and antimony (Table 2).

Staff et al. (2011) investigated the effects of Ga (III) coordination on human abdominal skin and porcine cheek skin using Franz cells. The dermal absorption of antimony *in vitro* has not been reported. The pharmacokinetics of antimony have been assessed in patients with leishmaniasis treated with an intramuscular sodium stibogluconate (pentavalent antimony) (Jaser et al., 1995). They found that antimony concentration remained lower in the skin than in blood for 4 h after treatment but increased after that. The previous and the present findings suggest that antimony has a

high affinity for the skin. Since antimony and arsenic are homologous metalloids, they might have similar chemical properties and affinities for tissues. Sodium arsenate has an affinity for thiol groups, and these are abundant in skin, hair, and nails that contain β-keratin, a sulfur-rich protein (Łoźna et al., 2014). Mann et al. (1996) showed that arsenic elimination via keratin represents As (III) binding to keratin in the skin, hair, and nails. The percutaneous absorption of As (III) and As (V) by artificial skin *in vitro* revealed that arsenic has a high affinity for keratinocytes: 1–10 % of the applied arsenic dose per hour was retained by the artificial skin (Bernstam et al., 2002). Like arsenic, antimony might also have a high affinity for keratin in the skin.

Histological observation has shown that inflammatory responses were not induced in pig skin exposed to GaSb for 24 h (Fig. 4). The toxic potential and inflammatory effects of GaSb were investigated in HDF cells cultured on thin films. We found that cytotoxicity was elevated after 3 and 7 days of exposure to GaSb (Fig.5).

Interleukins (IL-1β, IL-6, IL-8) and TNF-α are pro-inflammatory cytokines. Gasparrini et al. (2018) reported that pretreatment with strawberry extracts could reduce pro-inflammatory cytokines (TNF-α, IL-1β, and IL-6), which are related to anti-oxidant defense, in HDF. Yue et al. (2020) showed a remarkable increase in TNF-α and IL-6 mRNA levels following treatment with H_2O_2 in HepG2 cells, and pretreatment with

apigenin and bifendate significantly reduced the gene expression of TNF-α and IL-6. In this study, levels of IL-8 and pro-inflammatory cytokines did not increase after 1 and 3 days of exposure but were significantly elevated after 7 days compared to cells in the control group (Fig. 6). Similar to histological examination results, the inflammatory effect of GaSb is not obvious in HDF.

5. Conclusions

The present study investigated the dermal absorption of GaSb in pig skin *in vitro* for 24 h using Franz cells. Both gallium and antimony penetrated the skin, and permeation and resorption occurred for gallium. Histopathological findings did not reveal evidence of an inflammatory response in pig skin exposed to GaSb for 24 h. Cytotoxicity was significantly elevated after 3 and 7 days, and pro-inflammatory cytokines and IL-8 levels were low after 1 and 3 days but elevated after 7 days following the direct culturing of HDF on GaSb thin films. The short-term cytotoxicity and pro-inflammatory effect of GaSb on HDF were relatively low. Moreover, when GaSb thin films are applied as E-Skin devices, they are packaged or coated. Therefore, future temporal applications in epidermal optoelectronic devices with GaSb would be possible. Further studies are needed to evaluate the effects and toxicity of chronic exposure to GaSb.

Acknowledgments

This work was supported in part by JSPS KAKENHI grant number 17K19814 (Grants-in-Aid for Challenging Research (Exploratory)), awarded to J. F. We thank Editage (www.editage.com) for English language editing.

Conflict of interest

Neither of the authors has any conflicts of interest to declare.

References

Bernstam, L., Lan, C.H., Lee, J., Nriagu, J.O., 2002. Effects of arsenic on human keratinocytes: morphological, physiological, and precursor incorporation studies. Environ. Res. 89, 220–235. https://doi.org/10.1006/enrs.2002.4367

Bronaugh, R.L., Stewart, R.F., Congdon, E.R., 1982. Methods for *in vitro* percutaneous absorption studies. II. Animal models for human skin. Toxicol. Appl. Pharmacol. 62, 481–488. https://doi.org/10.1016/0041-008X(82)90149-1

Callewaert, C., Buysschaert, B., Vossen, E., Fievez, V., Van de Wiele, T., Boon, N., 2014. Artificial sweat composition to grow and sustain a mixed human axillary microbiome. Journal of Microbiological Methods. J. Microbiol Methods;103: 6-8. https://doi.org/10.1016/j.mimet.2014.05.005

Crosera, M., Prodi, A., Mauro, M., Pelin, M., Florio, C., Bellomo, F., Adami, G., Apostoli, P., De Palma, G., Bovenzi, M., Campanini, M., Larese Filon, F., 2015. Titanium Dioxide Nanoparticle Penetration into the Skin and Effects on HaCaT Cells. Int. J. Environ. Res. Public Health 12, 9282–9297. https://doi.org/10.3390/ijerph120809282

Crosera, M., Adami, G., Mauro, M., Bovenzi, M., Baracchini, E., Larese Filon, F., 2016. *In Vitro* Dermal Penetration of Nickel Nanoparticles. Chemosphere 145, 301–306. https://doi.org/10.1016/j.chemosphere.2015.11.076

Crosera, M., Mauro, M., Bovenzi, M., Adami, G., Baracchini, E., Maina, G., Larese Filon, F., 2018. *In vitro* permeation of palladium powders through intact and damaged human skin. Toxicol. Lett. 287, 108–112. https://doi.org/10.1016/j.toxlet.2018.02.009

Dutta, P.S., Bhat, H.L., Kumar, V., 1997. The physics and technology of gallium

antimonide: An emerging optoelectronic material. J. Appl. Phys. 81, 5821–5870. https://doi.org/10.1063/1.365356

EFSA, 2017. Guidance on dermal absorption, https://doi.org/10.2903/j.efsa.2017.4873

Franken, A., Eloff, F.C., Du Plessis, J., Badenhorst, C.J., Du Plessis, J.L., 2015a. *In vitro* permeation of platinum through African and Caucasian skin. Toxicol. Lett. 232, 566–572. https://doi.org/10.1016/j.toxlet.2014.12.010

Franken, A., Eloff, F.C., Du Plessis, J., Du Plessis, J.L., 2015b. *In Vitro* Permeation of Metals through Human Skin: A Review and Recommendations. Chem. Res. Toxicol., 28, 12, 2237–2249

Franz, T.J., 1975. Percutaneous absorption on the relevance of *in vitro* data. J. Invest. Dermatol. 64, 190–195. https://doi.org/10.1016/j.toxlet.2014.12.010

Fujihara, J., Nishimoto, N., 2020. Total antimony analysis by hydride generation-microwave plasma-atomic emission spectroscopy with applications. Microchemical Journal 157, 104992. https://doi.org/10.1016/j.microc.2020.104992

Gamer, A.O., Leibold, E., van Ravenzwaay, B., 2006. The *in vitro* absorption of microfine zinc oxide and titanium dioxide through porcine skin. Toxicol. in Vitro 20, 301–307. https://doi.org/10.1016/j.tiv.2005.08.008

Gasparrini, M., Giampieri, F., Forbes-Hernandez, T.Y., Afrin, S., Cianciosi, D., Reboredo-Rodriguez, P., Varela-Lopez, A., Zhang, J., Quiles, J.L., Mezzetti, B., Bompadre, S., Battino, M., 2018. Strawberry extracts efficiently counteract inflammatory stress induced by the endotoxin lipopolysaccharide in Human Dermal Fibroblast. Food Chem. Toxicol. 114, 128–140. https://doi.org/10.1016/j.fct.2018.02.038

Ivanoff, C.S., Ivanoff, A.E., Hottel, T.L., 2012. Gallium poisoning: A rare case report. Food Chem. Toxicol. 50, 212–215. https://doi.org/10.1016/j.fct.2011.10.041

Jaser, M.A., El-Yazigi, A., Kojan, M., Croft, S.L., 1995. Skin Uptake, Distribution, and Elimination of Antimony following Administration of Sodium Stibogluconate to Patients with Cutaneous Leishmaniasis. Antimicrob. Agents Chemother. 39, 516–519. https://doi.org/10.1128/AAC.39.2.516

Jung, H.H., Song, J., Nie, S., Jung, H.N., Kim, M.S., Jeong, J.W., Song, Y.M., Song, J., Jang, K.I., 2018. Thin metallic heat sink for interfacial thermal management in biointegrated optoelectronic devices. Adv. Mater. Technol. 3, 1800159. https://doi.org/10.1002/admt.201800159

Larese, F., Gianpietro, A., Venier, M., Maina, G., Renzi, N., 2007. In vitro percutaneous absorption of metal compounds. Toxicol. Lett. 170, 49–56. https://doi.org/10.1016/j.toxlet.2007.02.009

Larese Flion, F., Agostin, F.D'., Crosera, M., Adami, G., Bovenzi, M., Maina, G.,2008. *In vitro* percutaneous absorption of chromium powder and the effect of skin cleanser. Toxicol. *in Vitro* 22, 1562-1567. https://doi.org/10.1016/j.tiv.2008.06.006

Li, H., Xu, Y., Li, X., Chen, Y., Jiang, Y., Zhang, C., Lu, B., Wang, J., Ma, Y., Chen, Y., Huang, Y., Ding, M., Su, H., Song, G., Luo, Y., Feng, X., 2017. Epidermal inorganic optoelectronics for blood oxygen measurement. Adv. Healthcare Mater. 6, 1601013. https://doi.org/10.1002/adhm.201601013

Łoźna, K., Styczyńska, M., Bronkowska, M., Figurska-Ciura, D., Biernat, J., 2014. Arsenic contents in rats' fur as an indicator of exposure to arsenic. Preliminary studies. Rocz. Panstw. Zakl. Hig. 65, 287–290

Mann, S., Droz, P.O., Vahter, M., 1996. A physiologically based pharmacokinetic model for arsenic exposure. I. Development in hamsters and rabbits. Toxicol. Appl. Pharmacol. 137, 8–22. https://doi.org/10.1006/taap.1996.0052

Mauro, M., Crosera, M., Bovenzi, M., Adami, G., Maina, G., Baracchini, E., Larese Filon, F., 2019. *In Vitro* Transdermal Absorption of Al_2O_3 Nanoparticles. Toxicol. in Vitro 59, 275–280. https://doi.org/10.1016/j.tiv.2019.04.015

Nastiti, C.M.R.R., Mohammed, Y., Telaprolu, K.C., Liang, X., Grice, J.E., Roberts, M.S., Benson, H.A.E., 2019. Evaluation of Quantum Dot Skin Penetration in Porcine Skin: Effect of Age and Anatomical Site of Topical Application. Skin Pharmacol. Physiol. 32, 182–191. https://doi.org/10.1159/000499435

Nishimoto, N., Fujihara, J., Yoshino, K., 2017. Biocompatibility of GaSb thin films grown by RF magnetron sputtering. Appl. Surf. Sci. 409, 375–380. https://doi.org/10.1016/j.apsusc.2017.03.099

Nishimoto, N., Fujihara, J., 2019. Physicochemical and biocompatibility Analyses of surface-coated In0.57Sb0.43 thin films under aqueous conditions. Int. J. Mod. Phys. B 33, 1950109. https://doi.org/10.1142/S0217979219501091

Nishimoto, N., Fujihara, J., 2020. Characterization of GaSb thin films with excess Ga grown by RF magnetron sputtering. Int. J. Mod. Phys. B 34, 2050097. https://doi.org/10.1142/S0217979220500976

OECD, Test No. 428: Skin Absorption: In Vitro Method OECD Publishing, Paris (2004), https://doi.org/10.1787/9789264071087-en

Sato, K., Sugibayashi, K., Morimoto, Y., 1991. Species differences in percutaneous absorption of nicorandil. J. Pharm. Sci. 80, 104–107. https://doi.org/10.1002/jps.2600800203

Simon, G.A., Maibach, H.I., 2000. The pig as an experimental animal model of percutaneous permeation in man: qualitative and quantitative observations – an overview. Skin Pharmacol. Appl. Skin Physiol. 13, 229–234.

https://doi.org/10.1159/000029928

SCCS/1358/10: SCCS (Scientific Committee on Consumer Safety). Basic criteria for the in vitro assessment of dermal absorption of cosmetic ingredients. The SCCS adopted this opinion at its 7th plenary meeting of 22 June 2010.

Staff, K., Brown, M.B., Chilcott, R.P., Hider, R.C., Jones S.A., Kong X.L., 2011. Ga(III) complexes—The effect of metal coordination on potential systemic absorption after topical exposure. Toxicol. Lett. 202, 155–160. https://doi.org/10.1016/j.toxlet.2011.01.017

Sundar, S., Chakravarty, J., 2010. Antimony toxicity. Int. J. Environ. Res. Public Health 7, 4267–4277. https://doi.org/10.3390/ijerph7124267

Tang, H., Blankschtein, D., Langer, R., 2002. Prediction of steady-state skin permeabilities of polar and nonpolar permeants across excised pig skin based on measurements of transient diffusion: Characterization of hydration effects on the skin porous pathway. J. Pharm. Sci. 91, 1891-1907. https://doi.org/10.1002/jps.10177

Yue, S., Xue, N., Li, H., Huang, B., Chen, Z., 2020. Hepatoprotective Effect of Apigenin Against Liver Injury via the Non-canonical NF-κB Pathway *In Vivo* and *In Vitro*. Inflammation, 43, 1634-1648. https://doi.org/10.1007/s10753-020-01238-5

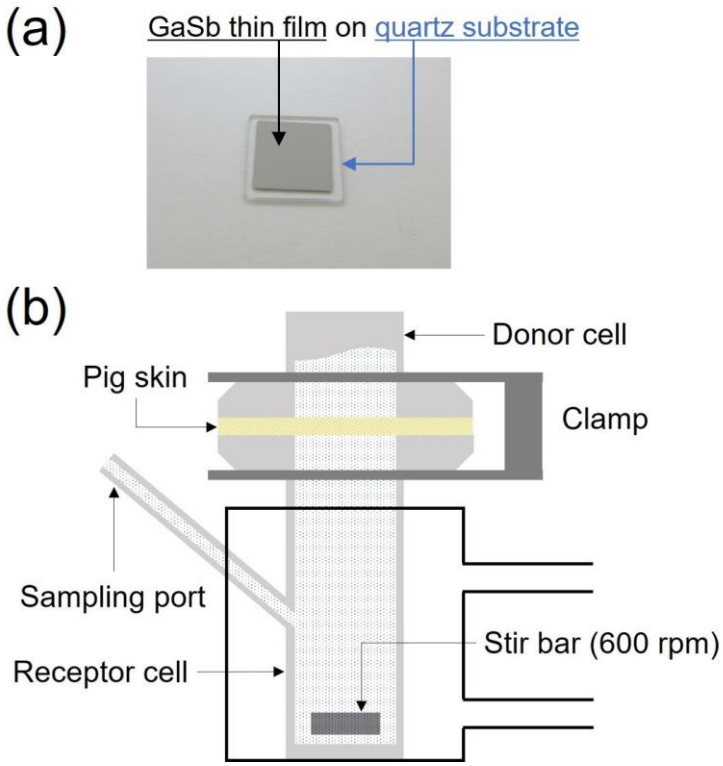

Fig. 1. (a) GaSb thin film on a quartz substrate. (b) Franz diffusion cell for experiments *in vitro*.

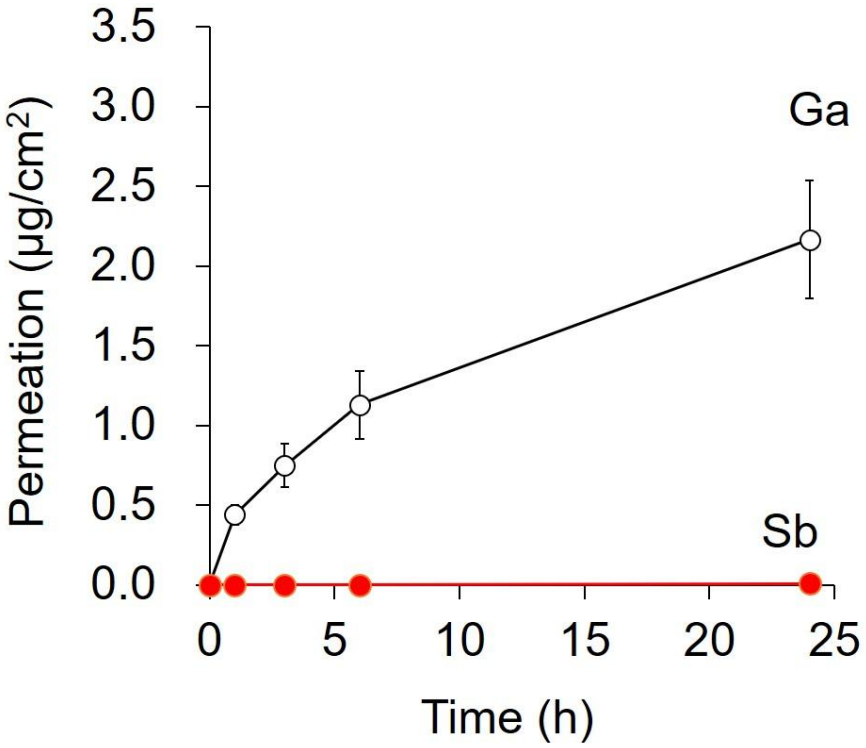

Fig. 2. Permeation profiles of gallium and antimony (mean ± SD) through pig skin (*n* = 6) exposed to GaSb soaked in synthetic sweat.

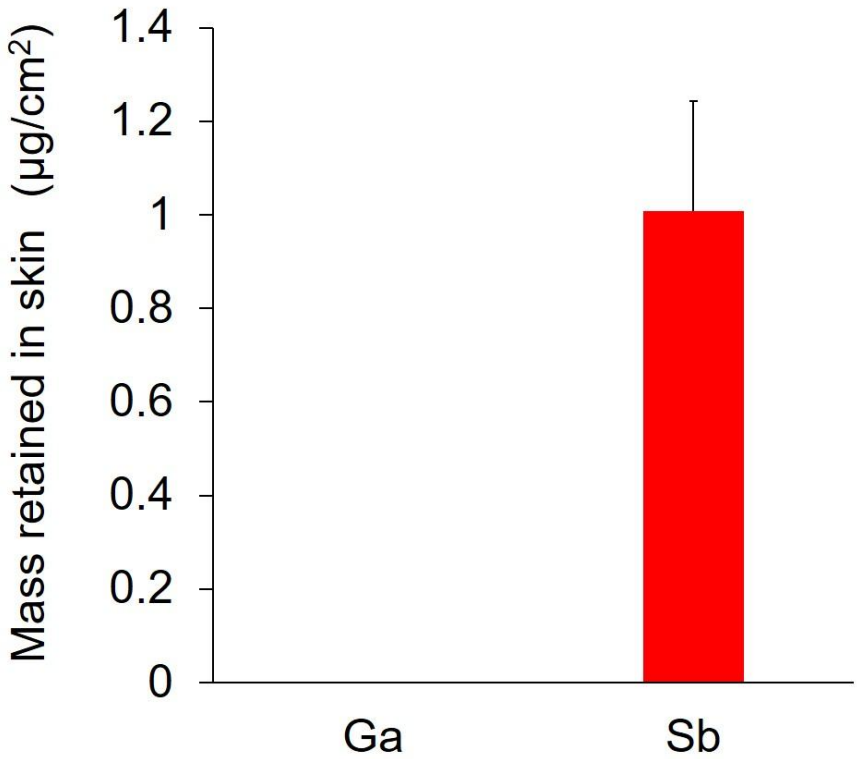

Fig. 3. Amounts of gallium and antimony (means ± SD) that penetrated pig skin (n = 6) exposed to GaSb soaked in synthetic sweat for 24 h.

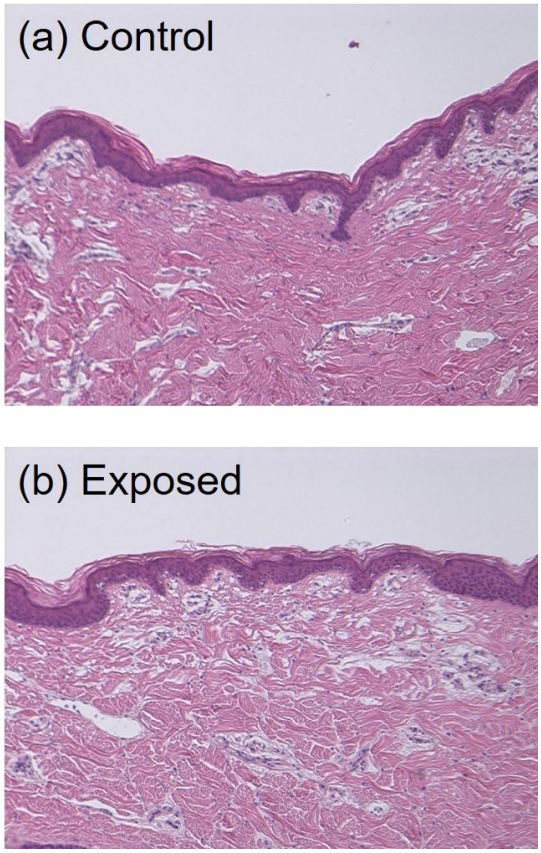

Fig. 4. Histopathological findings (HE, ×40 magnification) of pig skin. (a) Control. (b) Exposed to GaSb soaked in synthetic sweat for 24 h.

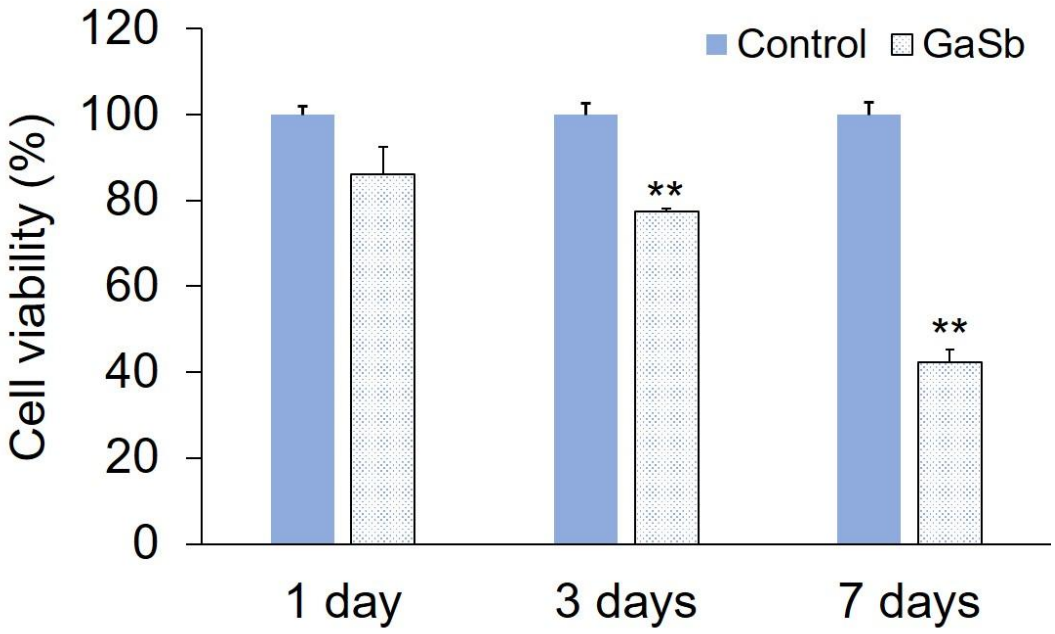

Fig. 5. Viability of HDF cultured directly on GaSb thin films. Cellular growth activities on days 1, 3, and 7 were assessed using MTT assays. Values are shown as means ± SD (n = 3). *p < 0.05; **p < 0.01 vs. control (Mann–Whitney U Test).

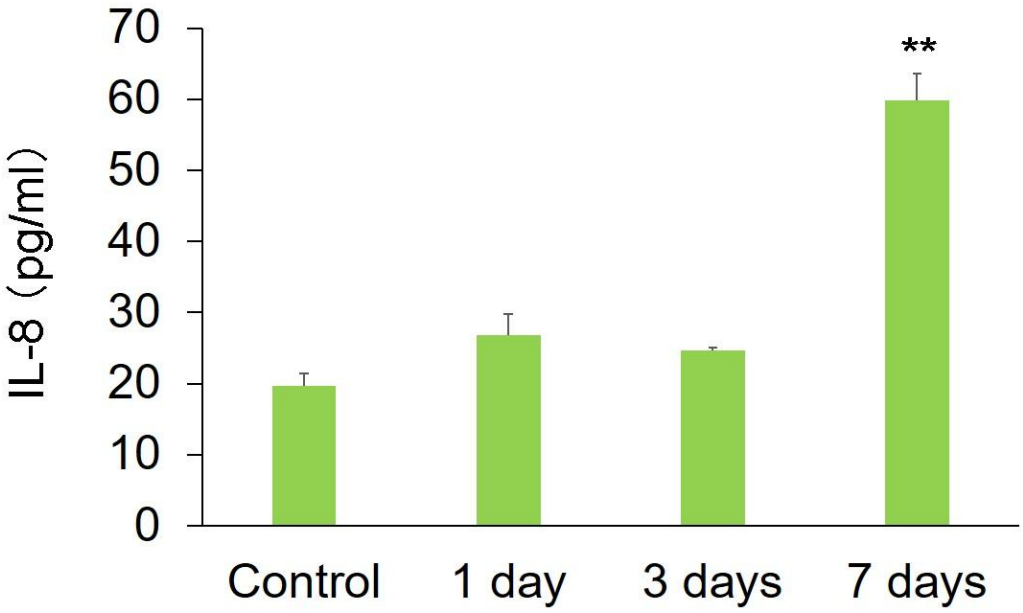

Fig. 6. IL-8 levels in HDF supernatants cultured directly on GaSb thin films after 1, 3, and 7 days of exposure. Data are shown as means ± SD (n = 3). **p < 0.01 vs. control (Dunnett's test).

Table 1. Method evaluation and recovery and precision of Ga and Sb in a skin sample spiked with Ga and Sb

	Ga	Sb
Calibration curve	$y = 16.9x + 43.2$, $r = 0.99988$	$y = 53.658x$, $r = 0.99996$
LOD (μg/L)	0.21	0.05*
LOQ (μg/L)	0.70	0.15*
N	3	3
added (μg/g)	36.1	36.1
found (μg/g)	36.4 ± 0.42	36.0 ± 1.30
Recovery (%)	101 ± 0.42	99.7 ± 3.60
RSD of intra-day assay (%)	0.42	2.37
RSD of inter-day assay (%)	3.14	3.61

r: correlation coefficient

LOD: limit of detection

LOQ: limit of quantification

The calculated formulas were LOD = $3\sigma/S$ and LOQ = $10\sigma/S$, respectively, where σ is the standard deviation from a blank after 10 measurements and S is the slope of the calibration curve.

RSD: relative standard deviation

* From our previous study (Fujihara et al., 2020)

Table 2. Mass balance of Ga and Sb in pig skin after 24 h exposure.

	Ga (µg/cm^2)	Sb (µg/cm^2)
Before exposure:		
Donor solution	5.69 ± 0.22	7.41 ± 0.09
After exposure:		
Residual metals in donor solution	3.93 ± 0.49	5.45 ± 0.27
Metals retained inside the Skin	< LOD	1.01 ± 0.24
Wash solution (residual metals on the skin surface)	0.05 ± 0.01	0.07 ± 0.05
Receptor solution	2.42 ± 0.18	< LOD
Recovery (%)	112	88

Data are shown as means ± SD (n = 6).

Ga: gallium

Sb: antimony

LOD: limit of detection